Nanomed. J. 9(3): 231-240, Summer 2022

RESEARCH PAPER

Novel chitosan-quinic acid nanoparticles labeled with m^{99} technetium for breast cancer imaging

Atousa Zia [1], Hakimeh Rezaei Aghdam [2], Mostafa Saffari [1], Jafar Farzaneh [2], Morteza Pirali Hamedani [3], Seyed Esmaeil Sadat Ebrahimi [4], Kimia Abdollahi [2], Saghar Sedigh Kheirabad [2], Fatemeh Zarringhalam [2], Farnoor Davachi omoomi [2], Ramin Farhoudi [4], Mehdi Shafiee Ardestani [2]**

[1]Faculty of Pharmacy, Islamic Azad University, Tehran, Iran
[2]Department of Radiopharmacy, Faculty of Pharmacy, Tehran University of Medical Sciences, Tehran, Iran
[3]Department of Medicinal Chemistry, Faculty of Pharmacy, Tehran University of Medical Sciences, Tehran, Iran
[4] Pasteur Institute of Iran

ABSTRACT

Objective(s): Today, cancer is one of the health concerns in modern societies. The use of nanoparticles in medical science has created new possibilities for diagnosis, imaging of tumors, and treatment of cancer in humans.

Materials and Methods: In this study, chitosan nanoparticles modified with quinic acid were used to diagnose breast cancer using a single-photon emission computed tomography imaging technique. For this purpose, quinic acid was activated by EDC/NHS and then binding was performed by adding chitosan nanoparticles.

Results: TEM, DLS, FTIR, and LC/MASS analyzes were used to investigate this conjugation. MTT toxicity test showed no toxicity on the HEK-293 cell lines and therapeutic properties for the MCF-7 cell line. The response surface method depends on the central composite design that was applied. For the highest labeling efficiency, using 3 factors: the amount of chitosan-quinic acid, pH, and SnCl2 as a reducing agent, and the efficiency of labeling was evaluated by thin-layer chromatography (TLC).

Conclusion: Finally, the study of biodistribution using SPECT imaging in cancer mice and its comparison with blocking tests showed that this compound has a good ability to diagnose breast cancer.

Keywords: *Blocking, Breast cancer, Chitosan, Quinic acid, SPECT imaging*

How to cite this article

Zia A, Rezaei Aghdam H, Saffari M, Farzaneh J, Pirali Hamedani M, Ebrahimi SES, Abdollahi K, Kheirabad SS, Zarringhalam F, Davachi omoomi F, Farhoudi R, Shafiee Ardestani M. Novel chitosan-quinic acid nanoparticlles labeled with m^{99} technetium for breast cancer imaging . Nanomed J. 2022; 9(3):231-240. DOI: 10.22038/NMJ.2022.64517.1673

INTRODUCTION

Breast cancer is the most common cancer in adult women worldwide and the second leading cause of death after lung cancer [1-3].

Factors influencing cancer include; being overweight [4], lack of physical activity [5, 6], alcohol consumption [6] , high-fat diet [7] cigarette [8] and tobacco smoke [9], high-risk genes and syndromes, personal history [10], family history [11], chronic inflammation, out of regulation night sleep [12] and hormonal imbalance, being female [13], long sexual cycle [14], low fertility and infertility [15, 16], taking contraceptives [17], consumption of Diethylstilbestrol [18], breast cellular changes, wounds and injuries [19], steroid hormones and their receptors [20, 21] and hormone replacement therapies [22].

There are different types of breast cancer inclusive of luminal type A and B, HER2 positive and pseudo basal [23].

Cancer staging indicates the rate of disease progression and is directly related to cancer mortality [24].

Molecular imaging plays an important role in the initial diagnosis, accuracy and precision of diagnosis, improvement of drugs and novel discoveries. In this regard, the use of SPECT for imaging is common. The detection sensitivity range for CT-scan and MRI imaging is about millimolar concentrations, but in SPECT the detection sensitivity range is picomolar concentrations. Also,

* *Corresponding authors: Emails: shafieeardestani@gmail.com; noora_dav@yahoo.com*

Note. This manuscript was submitted on March 21, 2022; approved on Jun 18, 2022

in CT and MRI imaging contrast is determined by the difference between tissue density and water volume, but in PET and SPECT contrast is obtained by determining a specific molecule labelled by one of the radioactive isotopes of its building blocks.

Technetium M99 is a radionuclide with a half-life of 6 hr, and the advantage of this radionuclide is its ability to emit gamma-ray with the energy of 192 Kev so it is widely used in nuclear medicine processes. Ascorbic acid and ferrous ion (Fe2+) were initially used as reducing agents but usually, the reduction was not complete and the unreactive protectants had to be removed.

Sodium borohydride ($NaBH_4$) and sodium dithionite (Na_2SO_4) which are effective in alkaline PH and Tin chloride that is commonly used in acidic PH, are some of the substances that can completely reduce Technetium.

Tin Chloride is capable of producing Technetium labelled compounds with high efficiency and does not require the removal of free protectant.

Other Tin salts such as Tin Fluoride and Tin Tartrate are also used in kits formulation.

chitin and chitosan are natural amino polysaccharides that show high biocompatibility, biodegradability, antibacterial and anti-allergic properties along with low toxicity [25]. Chitin has the chemical formula $(C_8H_{12}O_5N)n$ while Chitosan chemical formula is $(C_6H_{11}NO_4)n$. chitosan is a derivative of chitin. The number of acetyl groups on the polymer chain determines the difference between the two polymers. The polymer in which 100% of the amine groups is acetylated is called chitin and the polymer without any amide groups (100% amine groups) is called chitosan.

A polymer with less than 50% acetylation degree is conventionally called chitin whereas a polymer with more than 50% acetylation degree is called chitosan [26] (Fig. 1).

Chitin and chitosan are found in nature as alkaline substances which enable them to chemically bond fats, proteins, DNA, RNA and heavy metal ions.

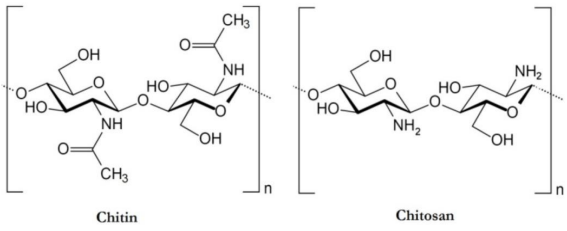

Fig. 1. Chemical structure of chitin and chitosan (26)

The main parameters affecting chitin and chitosan properties are molecular weight, degree of acetylation and crystallinity. In the discussion of pharmaceutical systems and human applications, also, the percentage of purity, moisture content and protein content should be considered [27].

Chitosan with suitable molecular weight can be eliminated by the kidneys in vivo, while very high molecular weight chitosan can be broken down into smaller pieces mainly by Chemical processes and enzymatic catalysts and then get removed by the renal clearance. Higher degree of acetylation causes a higher rate of chitosan decomposition. Decomposition by enzymatic catalysts also depends on the availability of chitosan amine groups. Chitosan is a safe and non-toxic polymer. The toxicity of chitosan increases with enlarging electrical charge density [28].

There are various techniques for preparing chitosan nanoparticles, including:

Ionic cross-links

Covalent cross-linking

There are several techniques for preparing particles such as emulsion, Ionotropic gelation, reverse micelles, solvent evaporation, dry spray, coagulation and sieving methods. During the preparation of these nanoparticles, a variety of Hydrophobic and hydrophilic drugs can be loaded into chitosan nanoparticles.

Deposition

There are two approaches for nanoparticle deposition. A solvent removal method in which the clotting agent (usually sodium sulfate) is added to an aqueous solution of chitosan. The solubility of chitosan is reduced through the combination of water and sodium sulfate. Another approach is based on the diffusion of emulsified solvent. Under the influence of emulsifying solvent, the aqueous phase containing chitosan disperses in the organic phase surrounding the drug. Then turbulence occurs between two phases and chitosan settles.

Polymerization

A dilute solution of nitric acid containing chitosan is stirred continuously with a mixture of ferric ammonium nitrate, nitric acid and isobutyl cyanoacrylate (at 40-celsius degrees for 40 minutes in an environment containing argon gas). After cooling to room temperature, sodium hydroxide is added to adjust PH to 5.4 and then

nanoparticle suspension is obtained.

For chemical conjugation of hydrophobic part, chitosan hydroxyl and amine groups with different synthetic pathways are used. By changing the substitution degree of the hydrophobic part, particles size and zeta potential can be easily controlled, which are important parameters in nanoparticles' biological distribution in the body. Various hydrophobic molecules such as bile acids (5-colanic acid, cholic acid and deoxycholic acid) and fatty acids (palmitoyl acid, stearic acid, oleic acid) have been used to develop the chitosan amphiphilic derivatives. Quinic acid is a cyclitol, cyclic polyol and cyclohexane carboxylic acid. It is a colourless solid that can be extracted from plant sources. Quinic acid also plays a part in the acidity of coffee.

Chitosan is mainly broken down by lysosomes and bacterial enzymes in the colon, and an absorbed portion of the nanoparticle is uptaken by macrophages and removed from the bloodstream. Binding between nanoparticles and macrophages is done by the adsorption of plasma proteins to the surface of nanoparticles, which is determined significantly by the surface charge of nanoparticles [29, 30].

MATERIALS AND METHODS

Synthesis of Nano conjugated chitosan-quinic acid

To synthesize nano conjugated, 30mg of quinic acid was dissolved in 10 ml of dimethyl sulfoxide/ water solution and 0.1 mmol of NHS/EDC was added as an additional activator, the lid was closed. The ≤reaction vessel was placed on a magnetic stirrer for 15 min and was stirred. Then 100 mg chitosan nanoparticle was added and was stirred again for 24-hr with a magnetic stirrer. Finally, the final product was dried using water, centrifugation and dialysis [29, 30].

Characterization

FTIR analysis

The FTIR spectrum was used to determine the functional groups in dendrimer. To prepare the spectrum after grinding a small amount of lyophilized conjugated sample with potassium bromide powder, the final powder is poured into a metal mattress and pressed with a hydraulic press. Then a clear tablet is formed which is used to assess the FT-IR spectrum by the intended machine. Finally, peaks appear on the screen and by identifying the functional groups, the sample structure is obtained.

Determination of the particle size

After sample delivery, preparation and photography for TEM analysis was performed by the operator following the above-mentioned items in day petronic laboratory. Image J software was used to estimate particle size.

DLS analysis

Under optimal laboratory conditions, a small amount of conjugated nanoparticle was poured into a glass vial with 1 ml of deionized water as the solvent. To ensure particle dissolution and transparency, the solution was filtered with a 0.5-micron filter and Sonicated for 10-minutes. It was then analyzed by a zeta sizer.

LC-mass analysis

Liquid chromatography _ mass spectrometry (LC-MS) is a combination of high-performance liquid chromatography (HPLC) and mass spectrometry methods.

As a result, many non-volatile and thermally unstable compounds, polar, ionic and large molecules can be analyzed through this method. In a liquid chromatography sample, the components are separated based on their molecular weight and their tendency to mobile and stationary phases, which leads to fragmentation of the sample and they transform to anions by losing H+ ions. The sample is then transferred into the empty chamber of the mass spectrometer. Next, the operation of the mass spectrometer is done according to their mass-charge ratio (m/z) by converting the analytic molecules to a charged (ionized) state.

With the subsequent analysis of ions and fragments generated during the ionization process.

Toxicity test

In this method, 100 µl of culture medium containing 30,000 cells in each well on a plate of 96 welled. After 24 hr of incubation, different concentrations of conjugated was added to cells and incubated for 72 hr in a CO_2 incubator, Then20 µl of MTT with a concentration of 5 mg/ml was added to each well and was incubated in the dark for another 4 hr. After the necessary time, the culture medium containing MTT was carefully removed and 200 µl of acidified isopropanol was added to each well to dissolve the purple formazan. After 15 min of incubation at room temperature,

each well was read by ELISA at 570 nm against a reference wavelength of 690 nm. For cell studies, HEK-293 and MCF-7 cell lines were used.

Cell survival rate (optimal absorption test/optical absorption control)

Results were reported based on average± the standard deviation using SPSS 15 statistical software. Data analysis was performed by student t-test. (P≤0.05).

Kit preparation

To prepare the kit, 10 mg of nano-conjugated with 1.8 mg of ascorbic acid was dissolved in 0.9 ml of double-distilled water and 30 µl of Tin chloride solution, then was lyophilized for 48 hr. To mark the kit, the required amount of activity was added to the vial in the amount of 1-5 ml and after sufficient time, the radiochemical purity was checked. For kit optimization, a central composite design (CCD) was used.

CCD

The response surface method, or RMS, is the use of mathematical and statistical methods to construct experimental designs of the process under consideration. In these methods, besides the main effect between factors, interactive (quadratic) effects and the interaction between the factors (interactions) can be estimated.

A complete description of a process with three effective factors, which has a quadratic behavior is given by the following equation:

$$Y=b0+b1x1+b2x2+b3x3+b12x1x2+b13x1x3+b23x2x3+b11x12+b22x22+b33x32$$

The central composite design is a common response surface methodology. The CCD method is similar to factor or fractional factor design, which comprises the central point and uses the star points to estimate the curve. The number of star points is double the number of factors (2k). CCD is normally designed in five levels, including +a, -1,0,1, -a (including three points within the specified range for each factor and two external points).

-1 and +1 are the upper and lower tiers and -a and +a are the new limitations of these factors. Zero is also the design center point. The exact value of Alpha (a) depends on the design characteristics and the number of factors. The value of Alpha is determined as follows and is dependent on the number of tests in the general CCD design component to maintain rotatability:

$$\alpha = [\text{Number of Factor design experiments}]^{1/4}=[2k]^{1/4}$$

As a result, the second equation holds for a complete factor design, where k denotes the number of factors.

Radiochemical quality control

Radiochemical quality control was performed by Whatman paper number 2 as a solid phase and two systems of 1:1 acetone/methanol as a solvent and saline solution as a mobile phase. To stain, about 5 µl of the labelled kit was taken and was stained at the distance of 1 cm from the bottom of the strip and was placed inside a chromatography tank. After about 10 cm moving of the mobile phase through the strip and drying, the paper was removed and was cut into 1 cm pieces, each piece was counted by a gamma well counter. In this case, if saline had been used, $m^{99}TCO_2$ would remain at the origin and labelled conjugated and $m^{99}TCO_2$ would move with the solvent front. If acetone/methanol had been utilized as the solvent, $^{99}mTCO_2$ labelled conjugated would remain at the origin and $m^{99}TCO_2$ would move with the solvent front, so the percentage of radiochemical purity could be determined from the following equation:

$$\text{Radiochemical purity}= 100 -(m^{99}TCO_2+m^{99}TCO_4-)$$

Injection of labelled material into mouse and imaging with SPECT

First, the mouse was anaesthetized with a small amount of ketamine/xylazine mixture. It was placed in a mouse compartment and 0.5 ml (about 1.4 mCi) of the final substance was injected into each mouse through the tail vein. After that, it was placed under the device in the form of supine. Tissue absorption was inspected by imaging of different tissues. Whole-body imaging was performed to see the post-injection condition in terms of transparency and contrast. The mouse was imaged 120 min after radiochemical injection. It was painlessly and urgently euthanized, following the ethical codes of working with laboratory animals, while still unconscious. Then with appropriate tools and in a suitable environment, the desired tissue was isolated and the amount of activity was determined using a dosing calibrator. Limbs weight was resolved by a scale. Then the activity of each tissue was calculated as a percentage of total activity per gram (%ID/g) on an average ±standard deviation.

For statistic study, SPSS, One way ANOVA and *Post-hoc* test Tukey was used.

RESULTS

FTIR analysis

Chitin and quinic acid surface groups were

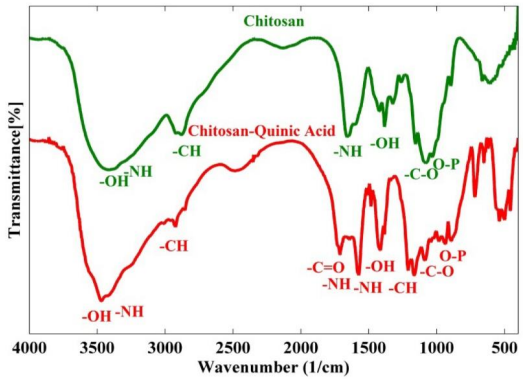

Fig. 2. FTIR spectrum of chitosan-quinic acid(red) and chitosan (green)

examined by FTIR. Peaks in the range of 3200-3500 cm^{-1} are assigned to amine and hydroxyl groups. peaks that appeared in 1703 cm^{-1} and 1484 cm^{-1} belong to the C=O and C-H groups, respectively, compared to chitosan nano conjugated. peaks in the region of 1340 cm^{-1} and 1120 cm^{-1} indicate the presence of the C=O and C-H and hydroxyl, Ester or ether functional groups sequentially. (Fig. 2, Table 1).

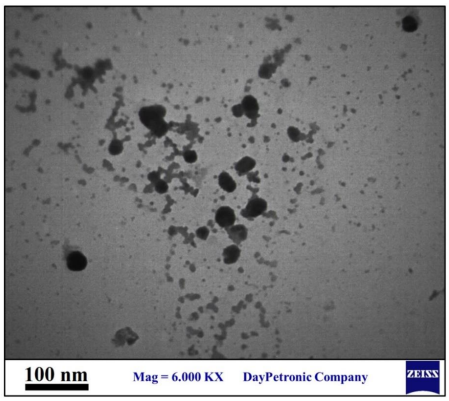

a

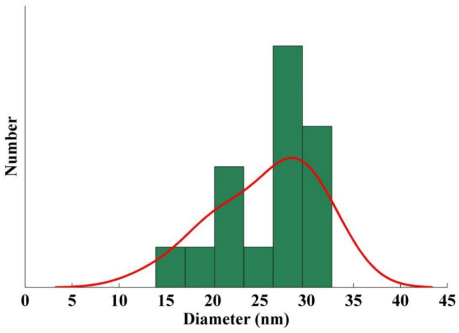

b

Fig. 3. a. TEM image of chitosan-quinic acid b. Particle size distribution of chitosan-quinic acid points

Table 1. FTIR spectrum results

Descriptor(cm^{-1})		
Quinic acid-chitosan	Chitosan nanoparticles	
3474	3423	-OH
3253	3273	-NH
2994	2879	-CH
1703	-	C=O
1636	1650	-NH
1583	1579	-NH
1484	1424	-CH
1417	1419	-OH
934	981	-OP

Structure characterization

The size and shape of the prepared nanoprobes were evaluated using the TEM imaging technique. TEM image attained from nanoprobes shows an almost spherical shape, with a size range of 15-34 nm and an average diameter of 25.69±5.37 (Fig. 3).

DLS results

The size of the chitosan nanoparticle was about 35 nm and was increased to 53 nm as a result of binding to quinic acid. The binding of quinic acid to these particles caused a 28 mv reduction in the zeta potential of the product (7 mv) to chitosan (35 mv) (Fig. 4).

LC-MASS analysis

LC-MASS analysis results are given below. Different fractures scrutinized indicate the

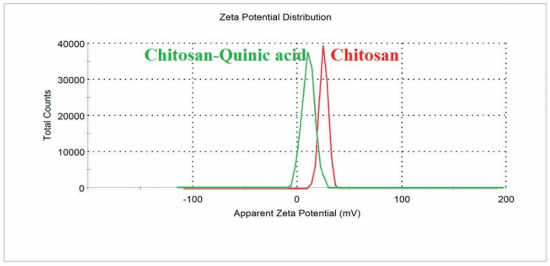

a

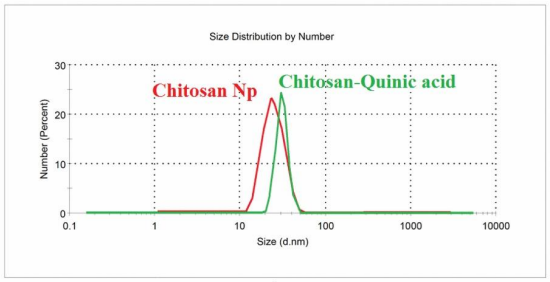

b

Fig. 4. a. Zeta potential spectrum of chitosan (red)and quinic acid (green) b. DLS spectrum of chitosan(red) quinic acid (green)

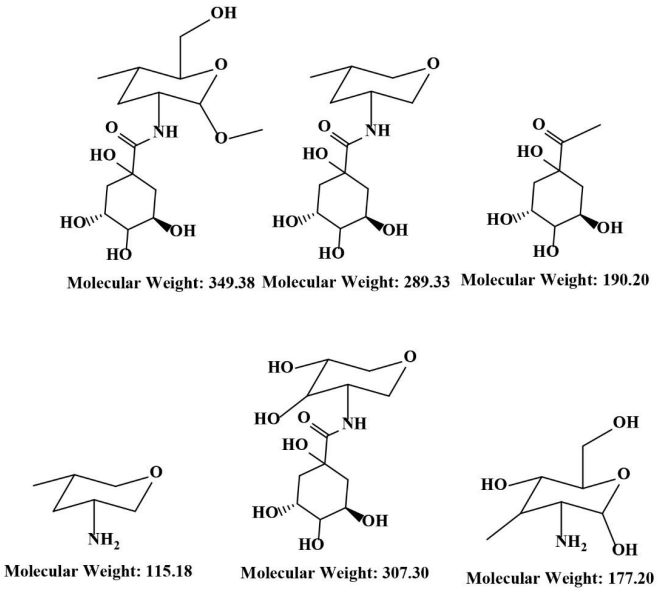

a

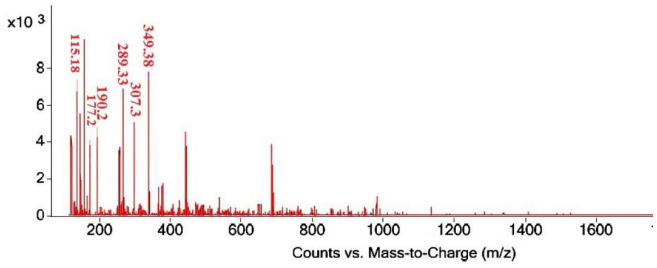

b

Fig. 5. a. Some fragments observed in mass. b. Chitosan mass spectrum (red) chitosan quinic acid (green)

successful binding of quinic acid to chitosan (Fig. 5).

Toxicity study

The toxicity of synthetic particle was analyzed on normal HEK-293 cells and MCF-7 cell line. MTT test outcome displayed no significant toxicity in none of the sample concentrations on any of the normal cells. (Fig. 6).

Optimization of labelling conditions

To provide the best labelling efficiency the effect of different parameters was considered. All of the variables were studied by the response surface method based on the central compound. To improve parameters influencing labelling and to achieve the highest faculty, three factors including pH, quinic acid-chitosan and the amount of reducing agent were tested in 5 levels (Table 2).

As can be seen from the table, items were

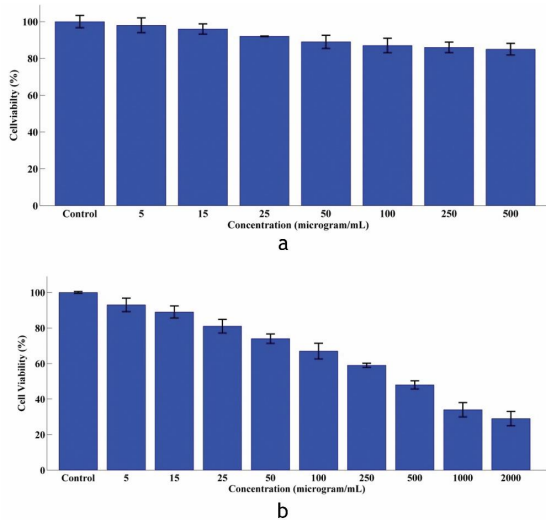

Fig. 6. a. Toxicity test result on MCF-7 cell line. b. Toxicity test results on HEK-293 cell line

Table 2. Examined parameters and coded values

Factor	Name	unit	-1.68	-1	0	1	1.68
A	pH	-	3.5	5	6.5	8	9.5
B	Reduced agent	mg	2	4	6	8	10
C	Chitosan-Quinic acid	mg	10	15	20	25	30

Table 3. Experimental design results

Test number	A	B	C	Percentage of labelling
1	-1	-1	1	70.1
2	0	0	0	91.95
3	-1	-1	-1	63.91
4	0	0	0	91.99
5	0	0	0	90.47
6	1	1	-1	86.22
7	-1.68179	0	0	73.11
8	0	0	1.68179	88.62
9	0	0	0	92.77
10	1.68179	0	0	90.89
11	1	-1	-1	81.69
12	0	0	0	91.7
13	0	1.68179	0	87.64
14	-1	1	1	94.41
15	0	-1.68179	0	79.3
16	0	0	-1.68179	71.25
17	0	0	0	92.4
18	1	1	1	94.85
19	-1	1	1	74.46
20	-1	1	-1	70.56

considered as follows; PH was selected in the range of 3.5 - 9.5, reducing agent in the range of 2 - 10 mg and chitosan-quinic acid in the range of 10 to 30 mg. central composite design was used based on expressed parameters with 5 repetitions for the central point. This plot allows the answers to be modelled by fitting in a mathematical equation. Twenty tests were performed and the conditions of each test and results are given in the Table 3.

Modelling was performed with three parameters, sentences resulting from binary multiplication between the main boundaries to consult the interaction between them and quadratic sentences of each main limits to consider the nonlinear relationship between response and main criterion. For further analysis, variance analysis was executed with a second-degree mathematical model. Variance analysis results on modelling are presented in the Table 4.

P-value <0.05 in the modelling process indicates the importance of each sentence effect. The results showed that except A*B interaction, other factors were important. Sign + demonstrates the direct relationship of the parameter and answer and sign - displays their inverse relationship and the magnitude of coefficient shows parameters

Table 4. Variance analysis results

Term	Coef	SE Coef	T-Value	P-Value	VIF
Constant	37.12	1.90	19.55	0.000	
A	5.97	1.35	4.44	0.001	1.12
B	3.31	1.35	2.46	0.034	1.12
C	4.37	1.38	3.16	0.010	1.20
A*A	-3.74	1.24	-3.01	0.013	1.05
B*B	-3.27	1.24	-2.63	0.025	1.05
C*C	-4.25	1.24	-3.42	0.007	1.05
A*B	-0.59	1.91	-0.31	0.764	1.35
A*C	0.11	1.10	3.06-	0.012	1.00
B*C	1.89	1.10	3.96	0.003	1.00

The resulting equation is as follows:
Y=37.12 + 5.97 A + 3.31 B + 4.37 C - 3.74 A*A - 3.27 B*B - 4.25 C*C- 0.59 A*B + 0.11 A*C + 1.89 B*C

Table 5. The final optimal value

Solutions				
Number	PH	Reduced Agent(mg)	Probe(mg)	MaxResp
1	7.3	8.3	22	95

greater effect. In this study, expanding each of the parameters increased the labelling.

Two-dimensional border views, the cooperation of effective parameters on the response can be discovered. These graphs show the simultaneous effects of two parameters on the response at a mean constant value of the third parameter. In these diagrams the minimum response to the maximum is shown as a blue to red colour change. In these studies, increasing of the values in interactions enhances efficiency, which is more extensive for the ligand. The optimal values of 4 variables based on the reduced model are given in the table of variance analysis results. (Table 5).

After obtaining the optimal value, the experiment was performed with 5 repetitions according to the above method.

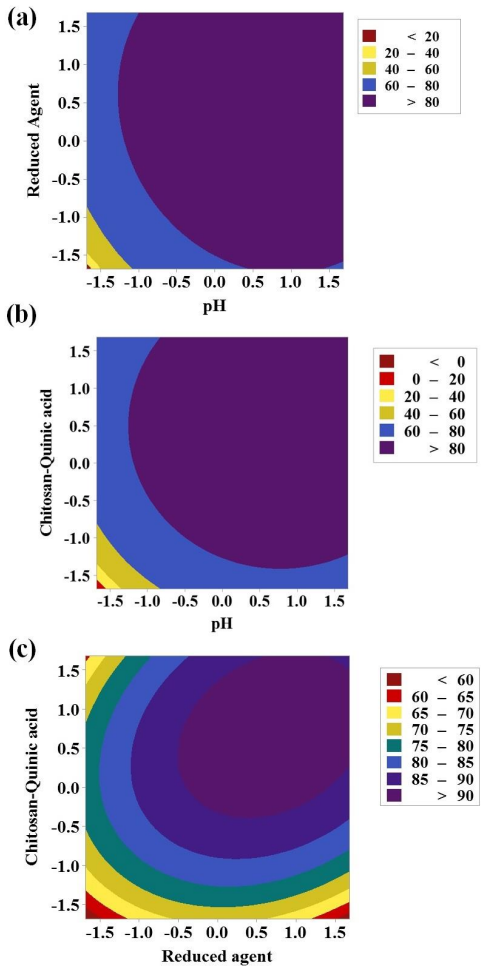

Fig. 7. a. Two-dimensional border of interaction between PH value and reducing agent. b. Three-dimensional spectrum of interaction between PH value and reducing agent. c. Two-dimensional border of interaction between PH value and adsorbent

Imaging results

Imaging results and analysis are displayed below. As can be seen, the synthetic particle has a good ability to detect cancer. Biodistribution results showed that in the cancer sample, it had accumulated about 9% while in the blocking sample this accumulation had decreased to 4%. This indicated the selectivity of this structure in breast cancer diagnosis. Compared to other cancerous tissue samples, aggregation in kidneys, liver and colon was elevated whereas in the spleen, lungs and heart was reduced (Fig. 8).

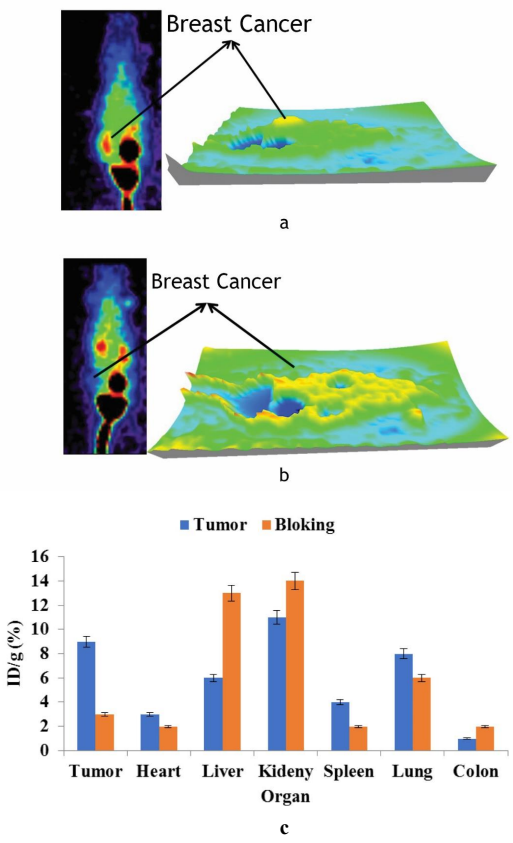

Fig. 8. a. Cancerous tissue imaging results. b. Blocking Imaging results. c. Biological distribution results in different organs

DISCUSSION

In this study, quinic acid was conjugated to chitosan nanoparticles for the first time and was used in cancer diagnosis. Quinic acid was activated by applying EDC/NHS and chitosan nanoparticles were used for binding. Conjugation is authenticated using DLS, TEM, FTIR, LC-MASS tests. MTT toxicity test was performed on cancerous cells (MCF-7) and normal cells (HEK-293) and compared between them. Finally, their ability to image cancerous tissue was evaluated.

The study puts forward to synthesize and evaluate the application of nano-conjugated chitosan-quinic acid for cancer diagnosis. Quinic acid based compounds were frequently used in recent literature to treat or find turmeric tissues as targeting agent and demonstrated very interesting results as our data were completely confirmed the literature results [21-26]. On the other hand quinic acid showed successful output in designing new interesting molecular imaging agents as well as therapeutic agents also theranostic compounds [21-26]. According to the findings of the present study, it is suggested that after confirming these outcomes and checking whether they can be used as a contrast agent to diagnose diseases and by conducting pathological studies in animals, this complex should be researched in human clinical phases. If the results of human clinical phases are accepted, most probably this product will enter the pharmaceutical market.

CONCLUSION

Based on the results it could be concluded that application of molecular targeting agent quinic acid is one of the successful strategies of delivery of radionuclides such as m99 Tc to cancerous tissue and developing such novel nanosized molecular imaging agents. Finally for better understanding and investigation of toxicological aspects of that molecule it is recommended to be assessed more preclinical and clinical data on this molecule in future studies.

ACKNOWLEDGMENTS

Tehran University of Medical Sciences International Campus supported this study. The authors would like to thank TPCF preclinical core of Tehran University for providing Imaging facility.

CONFLICT OF INTEREST

The authors declared no conflict of interest.

REFERENCES

1. Balekouzou A, Yin P, Pamatika CM, Bishwajit G, Nambei SW, Djeintote M, Ouansaba BE, Shu C, Yin M, Fu Z. Epidemiology of breast cancer: retrospective study in the Central African Republic. BMC Public Health. 2016;16(1):1-10.
2. Rojas K, Stuckey A. Breast cancer epidemiology and risk factors. Clin Obstet Gynecol. 2016;59(4):651-672.
3. Winters S, Martin C, Murphy D, Shokar NK. Breast cancer epidemiology, prevention, and screening. Prog Mol Biol Transl Sci. 2017;151:1-32.
4. Nyrop KA, Lee JT, Deal AM, Ki Choi S, Muss HB. Weight-related communications between oncology clinicians and women with obesity at early breast cancer diagnosis: findings from a review of electronic health records. Nutr Cancer. 2020;72(4):576-583.
5. Hidayat K, Zhou H-J, Shi B-M. Influence of physical activity at a young age and lifetime physical activity on the risks of 3 obesity-related cancers: systematic review and meta-analysis of observational studies. Nutr Rev. 2020;78(1):1-18.
6. Sun Q, Xie W, Wang Y, Chong F, Song M, Li T, Xu L, Song C. Alcohol consumption by beverage type and risk of breast cancer: A dose-response meta-analysis of prospective cohort studies. Alcohol Alcohol. 2020;55(3):246- 253.
7. Orange ST, Hicks KM, Saxton JM. Effectiveness of diet and physical activity interventions amongst adults attending colorectal and breast cancer screening: a systematic review and meta-analysis. CCC. 2021;32(1):13-26.
8. Kispert S, McHowat J. Recent insights into cigarette smoking as a lifestyle risk factor for breast cancer. Breast Cancer. 2017;9:127.
9. Sollie M, Bille C. Smoking and mortality in women diagnosed with breast cancer—a systematic review with meta-analysis based on 400,944 breast cancer cases. Gland Surg. 2017;6(4):385.
10. De Moulin D. A short history of breast cancer: Springer Science & Business Media; 2012.
11. Colditz GA, Kaphingst KA, Hankinson SE, Rosner B. Family history and risk of breast cancer: Nurses' health study. Breast Cancer Res Treat. 2012;133(3):1097- 1104.
12. Abubakar M, Sung H, Devi B, Guida J, Tang TS, Pfeiffer RM, Yang XR. Breast cancer risk factors, survival and recurrence, and tumor molecular subtype: analysis of 3012 women from an indigenous Asian population. Breast Cancer Research. 2018;20(1):1-14.
13. Group EHBCC. Body mass index, serum sex hormones, and breast cancer risk in postmenopausal women. Journal of the National Cancer Institute. 2003;95(16):1218-1226.
14. Barsotti Santos D, Ford NJ, Dos Santos MA, Vieira EM. Breast cancer and sexuality: The impacts of breast cancer treatment on the sex lives of women in Brazil. Cult Health Sex. 2014;16(3):46-257.
15. Johnson HM, Mitchell KB. Breastfeeding and breast cancer: Managing lactation in survivors and women with a new diagnosis. Ann Surg Oncol. 2019;26(10):3032- 3039.
16. Unar-Munguía M, Torres-Mejia G, Colchero MA, Gonzalez de Cosio T. Breastfeeding mode and risk of breast cancer: a dose–response meta-analysis. J Hum Lact. 2017;33(2):422-434.
17. Kamińska M, Ciszewski T, Łopacka-Szatan K, Miotła P, Starosławska E. Breast cancer risk factors. Prz Menopauzalny. 2015;14(3):196-202.
18. Hilakivi-Clarke L. Maternal exposure to diethylstilbestrol during pregnancy and increased breast cancer risk in daughters. Breast Cancer Research. 2014;16(2):1-10.
19. Boyd NF, Martin LJ, Bronskill M, Yaffe MJ, Duric N, Minkin S. Breast Tissue Composition and Susceptibility to Breast Cancer. Journal of the National Cancer Institute. 2010; 102(16): 1224-1237.

20. Kumar M, Salem K, Tevaarwerk AJ, Strigel RM, Fowler AM. Recent advances in imaging steroid hormone receptors in breast cancer. J Nucl Med. 2020;61(2):172-176.
21. Louie MC, Sevigny MB. Steroid hormone receptors as prognostic markers in breast cancer. Am J Cancer Res. 2017;7(8):1617.
22. Abdulkareem I. A review on aetio-pathogenesis of breast cancer. J Genet Syndr Gene Ther. 2013;4(142):2.
23. Holen I, Speirs V, Morrissey B, Blyth K. *In vivo* models in breast cancer research: progress, challenges and future directions. Dis Model Mech. 2017;10(4):359- 371.
24. Akram M, Iqbal M, Daniyal M, Khan AU. Awareness and current knowledge of breast cancer. Biol Res. 2017;50(1): 1-23.
25. Ali A, Ahmed S. A review on chitosan and its nanocomposites in drug delivery. Int J Biol Macromol. 2018;109:273-286.
26. Younes I, Rinaudo M. Chitin and chitosan preparation from marine sources. Structure, properties and applications. Mar Drugs. 2015;13(3):1133-1174.
27. Goy RC, BRITTO Dd, Assis OB. A review of the antimicrobial activity of chitosan. Polímeros: Ciência e Tecnologia. 2009;19(3):241-247.
28. Kean T, Thanou M. Biodegradation, biodistribution and toxicity of chitosan. Adv Drug Delive Rev. 2010;62(1):3-11.
29. Hu Y-L, Qi W, Han F, Shao J-Z, Gao J-Q. Toxicity evaluation of biodegradable chitosan nanoparticles using a zebrafish embryo model. Int J Nanomedicine. 2011;6:3351.
30. Mohammed MA, Syeda J, Wasan KM, Wasan EK. An overview of chitosan nanoparticles and its application in non-parenteral drug delivery. Pharmaceutics. 2017;9(4): 53.
31. Rezaei aghdam H, Bitarafan Rajabi A, Sadat Ebrahimi SE, Beiki D, Abdi K, Mousavi Motlagh SS , Kiani Dehkordi B, Darbandi Azar A, Shafiee Ardestani M. 18F-FDG MicroPET and MRI Targeting Breast Cancer Mouse Model with Designed Synthesis Nanoparticles. J Nanomater. 2022;5737835.